Available online at www.sciencedirect.com

ScienceDirect

Procedia Manufacturing 51 (2020) 771–778

Procedia MANUFACTURING

www.elsevier.com/locate/procedia

30th International Conference on Flexible Automation and Intelligent Manufacturing (FAIM2021)
15-18 June 2021, Athens, Greece.

A new structural two-component epoxy adhesive: Strength and fracture characterization

M.G. Cardoso[a,b], J.E.C. Pinto[a], R.D.S.G. Campilho[a,c,*], P.J.R.O. Nóvoa[a,c], F.J.G. Silva[a], L.D.C. Ramalho[c]

[a]*Departamento de Engenharia Mecânica, Instituto Superior de Engenharia do Porto, Instituto Politécnico do Porto, Rua Dr. António Bernardino de Almeida, 431, 4200-072 Porto, Portugal*

[b]*Departamento de Engenharia Mecânica, Faculdade de Engenharia da Universidade do Porto, Rua Dr. Roberto Frias, s/n, 4200-465 Porto, Portugal*

[c]*INEGI – Pólo FEUP, Rua Dr. Roberto Frias, s/n, 4200-465 Porto, Portugal*

* Corresponding author. Tel.: +351 939 526 892; fax: +351-228-321-159. *E-mail address:* raulcampilho@gmail.com

Abstract

In the past decades, adhesive technology has been useful in order to solve numerous issues related with conventional joining techniques (bolting, riveting and welding). Several advantages of adhesive bonding can be pointed out, such as low weight (relevant in the automotive and aeronautical industries), capability to resist to adverse environmental conditions, lower manufacturing costs and possibility to join different materials. To predict crack propagation of an adhesive joint by advanced fracture mechanics-based techniques such as cohesive zone models (CZM) it is not enough to know the traditional mechanical properties, such as Young's modulus (E), shear modulus (G), tensile strength (σ_f) and shear strength (τ_f). Actually, it is also mandatory to estimate the tensile (G_{IC}) and shear fracture energies (G_{IIC}). The purpose of this work is to carry out the mechanical and fracture property characterization of a new structural two-component epoxy adhesive. With this purpose, four tests which were conducted: tensile testing to bulk specimens, shear testing with thick adherend shear tests (TAST), double-cantilever beam (DCB) and end-notched flexure (ENF). With these tests, it was possible to determine the mechanical and fracture properties of the adhesive in tension and shear. Different data reduction methods were evaluated for the fracture properties. The test results agreed with the data provided by the manufacturer and will enable the design of bonded structures with this adhesive.

© 2020 The Authors. Published by Elsevier Ltd.
This is an open access article under the CC BY-NC-ND license (https://creativecommons.org/licenses/by-nc-nd/4.0/)
Peer-review under responsibility of the scientific committee of the FAIM 2021.

Keywords: Structural adhesive; Bulk specimens; Thick Adherend Shear Test; Fracture toughness.

1. Introduction

Adhesive joints allow achieving structures with a lower weight, are capable to join different materials, present high fatigue strength, among others advantages [1]. For a proper joint design, it is necessary to estimate the properties of the adhesives, as these widely vary between types of adhesives. These properties are also decisive to predict the stress distributions and choose proper failure criteria, as well as they are essential to predict the joint strength [2, 3]. The bonding technology is recommended for composite materials because it is difficult to joint composites with traditional methods. Drilling composite materials by screwing or riveting could damage the composite structure, which is harmful to the material's strength and durability. Furthermore, the drilled hole needs to be sealed, by application of a complex technique, to avoid delaminations [4]. It is also necessary to take into account environmental effects, especially regarding moisture, as composite structures can absorb moisture, which can seriously affect the mechanical properties and can even lead to degradation of the fibres, especially in the drilling holes [5]. With the increasing use of these materials, the adhesive bonding

2351-9789 © 2020 The Authors. Published by Elsevier Ltd.
This is an open access article under the CC BY-NC-ND license (https://creativecommons.org/licenses/by-nc-nd/4.0/)
Peer-review under responsibility of the scientific committee of the FAIM 2021.
10.1016/j.promfg.2020.10.108

technology also evolved. A bonded joint is basically subjected to peel and shear loads. Thus, to predict the joint's behaviour, the knowledge of the (E), the (G), the (σ_f) and the (τ_f) is not enough. For advanced modelling techniques such as CZM, the fracture toughness in pure mode I (G_{IC}) and pure mode II (G_{IIC}) are also required. In order to entirely characterize an adhesive, it is thus necessary to quantify all these parameters by performing specific tests [6]. Different options exist to predict the tensile properties of an adhesive, either tests using bulk adhesive samples or adhesive joint tests. The butt joint is an option to estimate the tensile properties of adhesives. Performing bulk tensile tests is another alternative to estimate the tensile adhesive properties [7]. Bulk samples can be obtained by the closed-mould technique or by pressure between plates, this last technique applicable in the presence of relatively stiff and brittle adhesives. Banea and da Silva [8] used the plate-to-plate method when fabricating bulk samples of stiff and brittle epoxy adhesives, the Araldite® AV118 and the Nagase Chemtex® XN1244. Adhesive joints should be preferably designed to work in shear, considering that the loads are distributed across a more extensive area than in peel. The shear tests also can be divided into bulk joint and adhesive tests. When the adhesive joint testing is performed, it is quite difficult to precisely measure the shear displacement because the values of this displacement are very small. Bulk samples have a longer measurement length, so it is possible to achieve better results, but it can be argued that the size and thickness of the samples are not representative of the adhesive properties in a joint. To determine the shear mechanical properties, the most usually used tests are the TAST, Iosipescu or V-notched shear beam test, butterfly test or notched shear plate method (Arcan), bulk test in torsion, butt joint torsion test or Napkin Ring, and single-lap joint (SLJ) test. Between all these tests, the most accurate is the torsion test due to the absence of stress concentrations [9]. This test exhibits as the main difficulty the need to have a specific torsion device. Banea et al. [10, 11] used the TAST configurations, which enabled to characterize the shear properties from different adhesives and accomplish the respective validation.

Nowadays, advanced strength prediction methods for bonded joints are popular, but these additionally require the knowledge of fracture properties of adhesives. Classic fracture mechanics requires a crack in the structure, induced during the manufacturing process or produced when the structure is loaded [12]. Using this method to estimate the strength of adhesive joints reveals some significant advantages over the strength materials methods [11]. However, application of classical fracture mechanics techniques supposes the existence of an initial flaw in the structure to be analysed, which many times does not exist in reality [12]. The CZM technique is also based on fracture parameters such as G_{IC} or G_{IIC}, but damage onset is actioned by stress parameters, so these advanced techniques do not need an initial crack to trigger damage propagation [13]. The Tapered Double-Cantilever Beam (TDCB) and the DCB are the most common tests used to estimate G_{IC} [7, 14], which procedure is extensively described in the standard ASTM D 3433-99 [15] and recently implemented in the standard ISO 252117: 2009 [16]. In the work developed by Blackman et al. [17], different materials were selected to be used as adherends to perform DCB and TDCB tests, to compare the G_{IC} values of a brittle adhesive. In the DCB tests, the adherends used were unidirectional carbon-fiber composite and mild steel. In the TDCB tests, the adherends used were mild steel and aluminium alloy. It was concluded that the resulting G_{IC} values by different data reduction methods were identical, although dependent on the adherend material. The easiest and most commonly used test for shear characterization of bonded joints is the ENF. However, there are many other tests that could be used in order to predict G_{IIC}, such as the End-Loaded Split (ELS) and the Four-Point End-Notched Flexure (4ENF). For two different adhesives, DCB and ENF tests were performed by Banea and da Silva [10] and Banea et al. [18] to obtain G_{IC} and G_{IIC}, respectively. It was concluded that the DCB and ENF tests are reliable in obtaining G_{IC} and G_{IIC} of adhesive joints, respectively, for further application in Fracture Mechanics and Damage Mechanics techniques for adhesive joint design. Full characterization of a new epoxy adhesive with high elongation and toughness (XNR6852 by Nagase Chemtex®) was undertaken by Saldanha et al. [19]. In order to achieve the total characterization of the adhesive, mechanical and fracture static tests, impact tests and glass transition temperature (T_g) measurements were implemented. The obtained results exhibit high values for σ_f and τ_f, typical of an epoxy adhesive, and high elongation, typical of a polyurethane adhesive. Thus, it could be concluded that the XNR6852 combines the best peculiarities of an epoxy and a polyurethane adhesive. The measurement of the fracture properties as a function of the mode-mixity was undertaken in other works [20], allowing the calculation of the fracture envelopes, which find application in the strength prediction by CZM modelling. Azari et al. [21] characterized the mixed-mode fracture behaviour of a toughened epoxy adhesive by the DCB specimens, using a constructed apparatus that enabled loading the specimens with different forces at each adherend. The resulting properties from this procedure allowed to predict the strength of cracked-lap shear and single-lap joints by accessing the developing fracture energies and comparing them with the previously defined mixed-mode properties at a specific mixed-mode condition. Validation was undertaken against experimental data, with good results.

The purpose of this work is to carry out the mechanical and fracture property characterization of a new structural two-component epoxy adhesive. With this purpose, four tests which were conducted: tensile testing to bulk specimens, shear testing with TAST, DCB and ENF tests. With these tests, it was possible to determine the mechanical and fracture properties of the adhesive in tension and shear. Different data reduction methods were evaluated for the fracture properties.

2. Experimental tests

2.1. Tensile tests

To perform the bulk specimens with dogbone shape for tensile testing, a mould was used that allows obtaining six specimens at once. The mould was developed and fabricated to reproduce specimens according to the indications and dimensions described in the French Standard NF T 76-142 [22, 23]. A CNC milling machine was used in order to fabricate the

top and bottom plates from the mould. Furthermore, the plates were surface grinded to guarantee a perfect surface finish and subjected to hard chrome plating to increase the abrasion resistance, as well as to ease the specimens' demoulding. Laser cutting was used to manufacture the intermediate plate. Both processes chosen to manufacture the mould are extremely accurate and work with low tolerances. The process began with the mould preparation, and it was necessary to clean with acetone the different parts that constitute the mould, followed by application of demoulding agent. After the mould is ready, it was necessary to prepare the adhesive (SikaPower® 1277) according to the manufacturer's specifications, manually fill the six mould cavities and finally close the mould for adhesive curing during one week (Fig. 1). The specimens were tested in a Shimadzu AG-X 100 testing machine, equipped with a 100 kN load cell, at room temperature and with a test velocity of 2 mm/min. Strain measurement was undertaken by using a mechanical extensometer with a base length of 50 mm (**Erro! A origem da referência não foi encontrada.**).

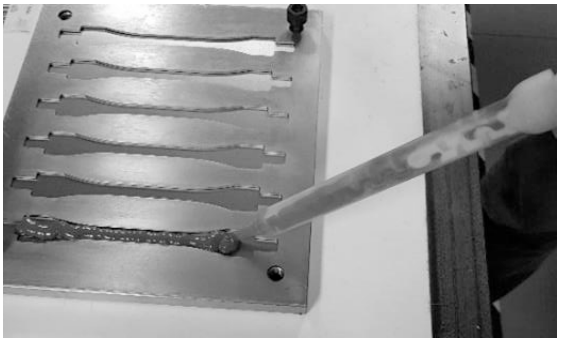

Fig. 1 – Manufacturing the bulk specimens (adhesive application).

Fig. 2 –Bulk test setup with the mechanical extensometer positioned.

2.2. Shear tests

Concerning the adherends used to perform the shear tests, in-house developed TAST adherends and tools were used (Fig. 3). The TAST specimens were fabricated in C45E steel with geometry and dimensions according to the ISO 11003-2 standard [24]. The first step to prepare the adherends was to sandblast them and to remove traces of oil and dust. After, it was necessary to clean the adherends with acetone. In order to accomplish the intended value of overlap length, 1 mm thick blades were used as spacers between the adherends. The blades and all mould surfaces were properly prepared with demoulding agent to facilitate the extraction process after bonding the specimens. After the application of the adhesive into adherends, these were manually positioned, the joints pressed, and the limiting bars were fastened to the jig by screws to guarantee perfect specimens' alignment. The adherends were cured according to manufacturer's recommendations. In all specimens, the bonding area was 25×5 mm^2 and the adhesive thickness was 0.7 mm. During the test, a mechanical extensometer was used to measure the longitudinal strains. Following the ISO 11003-2 standard for TAST tests [24], a speed of 0.5 mm/min was used.

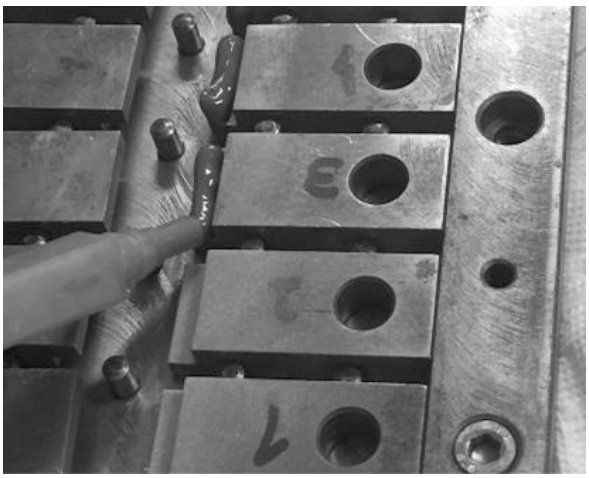

Fig. 3 – Manufacturing TAST specimens (adhesive application).

2.3. Fracture tests

In order to predict G_{IC} the DCB test specimen was undertaken (Fig. 4 (a)), meantime to estimate G_{IIC} the ENF (Fig. 4 (b)) was selected. The adherends were composed of aluminium alloy sheet (AA6082 T651). The adherends' dimensions for DCB testing were 140×25×3 mm^3, and the ENF adherends' dimensions were 230×25×3 mm^3. Campilho et al. [11] characterized this material and the following parameters were found: E=70.07±0.83 GPa, tensile yield stress σ_y=261.67±7.65 MPa, σ_f=324±0.16 MPa and tensile failure strain ε_f=21.70±4.24%. The specimens for the DCB test were prepared with following dimensions: total length (L) of 140 mm, initial crack length (a_0) of approximately 50 mm, adherend thickness (t_P) of 3 mm, width (b) of 25 mm and adhesive thickness (t_A) of 1 mm. The dimensions for the ENF tests are: L of 230 mm, mid-span (L_1) of 100 mm, initial crack length (a_0) of approximately 65 mm, adherend thickness (t_P) of 3 mm, width (b) of 25 mm and adhesive thickness (t_A) of 1 mm. All adherends had to be prepared prior to the bonding process. The surfaces to be bonded were sandblasted, cleaned and

degreased with acetone. Due to the known variations of G_{IC} and G_{IIC} with t_A induced by different constraints between the adhesives, it is important to ensure a constant value of t_A throughout the bonding. To achieve this goal, spacers were used between the adhesives to control t_A [24]. In order to induce the crack tip a spacer was inserted, and it was composed by a 0.1 mm thick razor blade between the calibrated bars to guarantee a sharp crack tip. Following the manufacturer's indications, curing was performed at room temperature for one week. To ensure the correct positioning of the spacer and avoid misalignment, the joints were cured in a steel mould.

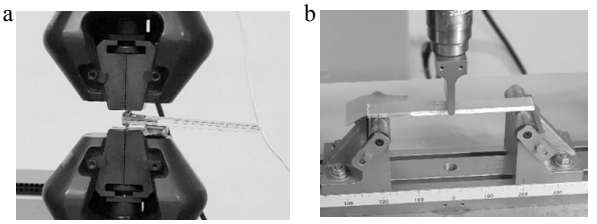

Fig. 4 - Setup of the fracture tests: DCB (a) and ENF (b).

3. Methodology

3.1. Tensile tests

To determine the tensile mechanical properties of the adhesive, the standard EN ISO 527-2 [25] was adopted. The value of E was measured as the average slope of the stress-strain (σ-ε) curve between elastic strains of 0.05% and 0.25%. σ_y was obtained for a strain of 0.2%, by the intercept between the stress-strain (σ-ε) curve and a parallel line to the initial part of this curve. σ_f is calculated by the ratio between the maximum load and the initial cross-section of the specimen. The value of ε_f, which corresponds to complete failure, was also assessed [26].

3.2. Shear tests

The calculation of the shear stress (τ) was given by $\tau=P/(l\times b)$, where the applied load is defined by P, b is the width and the bonded length is defined by l. The applied displacement (δ) divided by t_A gives the shear strain (γ). Lastly, the ratio τ/γ in the elastic zone of the τ-γ curve give the estimation of G [27]. In order to determine all the described mechanical shear properties of the adhesive, the ISO 11003-2 standard [24] was considered.

3.3. Mode I fracture tests

In order to evaluate G_{IC}, the following data reduction methods were used: Compliance Calibration Method (CCM), Corrected Beam Theory (CBT) and Compliance-Based Beam Method (CBBM). Campilho et al. [28] detailed the theoretical background of these three formulations, all of them considering the fracture process zone (FPZ) near the crack tip. The CCM is founded on the Irwin-Kies [29] equation, being fundamentally based on the specimen's compliance ($C=\delta/P$). A crack length correction (Δ) is used in CBT, in order to include the crack tip rotation and deflection in the analysis, obtained as specified in ISO 15024 [30]. The CBBM is considered a relatively simple but robust method based on an equivalent crack length (a_{eq}), and it only depends on the specimens' compliance measured during the course of the test [28].

3.4. Mode II fracture tests

The chosen adhesive presents a large ductility, which makes it difficult to measure the real a. In order to evaluate G_{IIC}, the CCM, CBT and CBBM data reduction methods were used. As previously mentioned, the CCM is based on the specimens compliance and the Irwin-Kies equation [29]. Wang and Williams [31] proposed the CBT to measure G_{IIC}, which includes crack length corrections to account for the effects of shear deformation. The CBBM, by using the a_{eq} concept, allows the G_{IIC} estimation from the readily available parameters after experimental testing, i.e. P and δ (which provide C) [32]. This method is known to account for the FPZ at the crack tip by using a_{eq} instead of a. Further details of the method can be founded in the work of de Moura et al. [33].

4. Results

4.1. Tensile tests

The failure modes have been documented, and smooth failure surfaces without porosities were found in all specimens.

Fig. 5 shows the σ-ε curves obtained in the bulk tensile tests, being visible non-negligible deviations in σ_f and especially ε_f. These differences could be due to experimental fabrication and/or testing issues. However, all failures were valid without visible defects on the fractured surfaces and, thus, all specimens were considered in the data analysis.

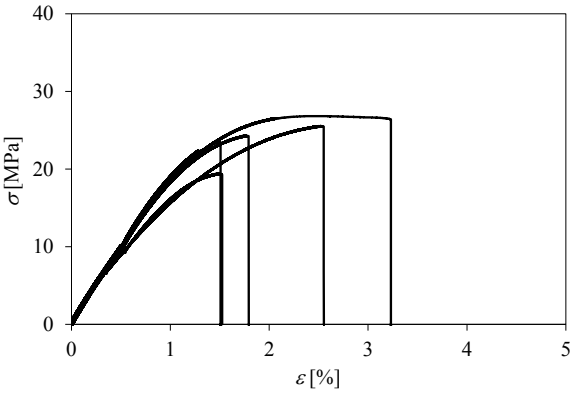

Fig. 5 - σ-ε curves of bulk testing.

Table 1 presents the individual and average tensile properties of the adhesive, where the maximum load is represented by P_m and the maximum displacement is represented by δ_f.

Table 1 - Individual and average tensile properties of the adhesive.

Specimen	P_m [N]	E [MPa]	σ_y [MPa]	σ_f [MPa]	ε_f [%]
4	496.28	1780.86	18.41	19.43	1.52
5	630.11	2010.61	21.96	26.36	3.23
6	603.93	2185.35	21.03	23.50	1.51
7	641.03	2014.14	14.90	25.56	2.55
8	615.74	2067.85	20.76	24.32	1.79
Average	597.42	2011.76	19.41	23.83	2.12
Standard Deviation	58.26	147.14	2.84	2.70	0.75

4.2. Shear tests

All TAST specimens revealed that the failure surfaces were cohesive, and the topology of the fractured surfaces was identical. When analysing the τ-γ curves (Fig. 6) obtained from TAST testing, higher repeatability between the specimens is observed on all relevant parameters. The shear yield stress (τ_y) was assessed by the interception between the τ-γ curve and a straight line parallel to the initial slope of the τ-γ curve for γ=0.2%. Table 2 shows the relevant data obtained during the tests and the respective shear mechanical properties of the adhesive.

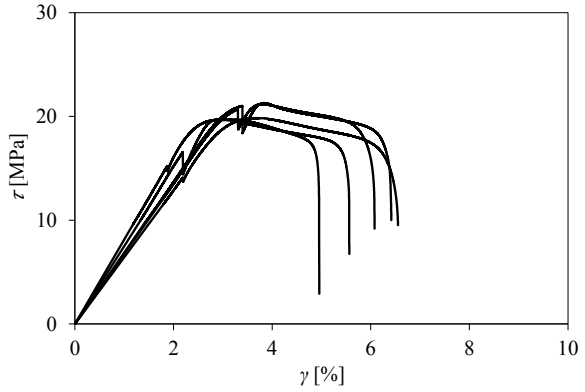

Fig. 6 - τ-γ curves of TAST testing.

Table 2 - Individual and average shear properties of the adhesive.

Specimen	P_m [N]	G [MPa]	τ_y [MPa]	τ_f [MPa]	γ_f [%]
1	2661.36	690.00	20.56	21.29	6.42
2	2459.64	790.00	19.50	19.68	5.56
3	2649.63	675.00	20.54	21.20	6.08
4	2481.10	660.00	19.10	19.85	6.55
5	2467.98	750.00	19.67	19.74	4.96
Average	2543.94	713.00	19.87	20.35	5.91
Standard deviation	102.20	54.95	0.65	0.82	0.66

4.3. Mode I fracture tests

After the tests, the failure surfaces of the six DCB specimens were documented, and it could be concluded that all failures were cohesive (Fig. 7).

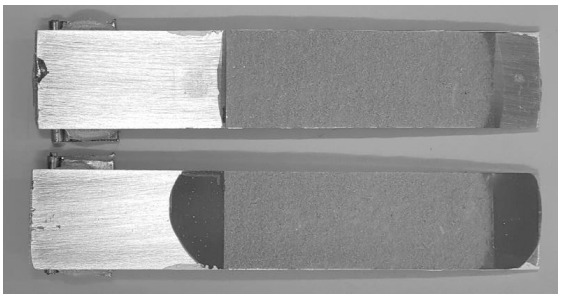

Fig. 7 - DCB specimen after testing.

The P-δ curves of the DCB tests (Fig. 8) initially present a linear increase of P. After crack growth onset a relaxation of P is visible, corresponding to crack propagation at a constant value of the tensile strain energy release rate (G_I). The results of DCB testing exhibited a high repeatability in the P-δ curves, both before crack initiation and during crack growth. The estimation of the C=f(a) curve and its differentiation are necessary to obtain G_I by the CCM. In order to correctly estimate G_{IC}, the C=f(a) curve must be analysed between the beginning of crack propagation and before complete failure of the specimens. Fig. 9 compares the R-curves, which relate the evolution of G_I with a or a_{eq} [34], between the CCM, CBT and CBBM for a single DCB specimen. Crack propagation took place with an approximate steady-state value of G_I during the DCB tests. However, some experimental deviations occurred due to the natural deviations in adhesive properties, experimental issued and possible localised adhesion defects [20].

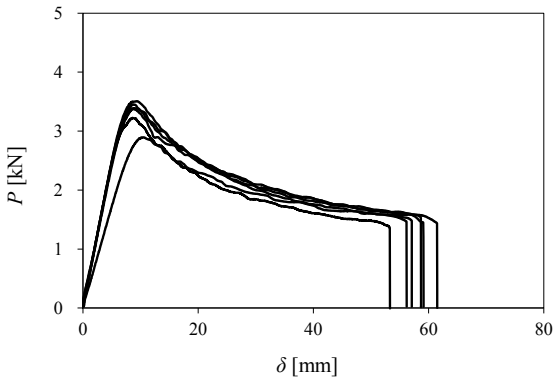

Fig. 8 – P-δ curves of DCB testing.

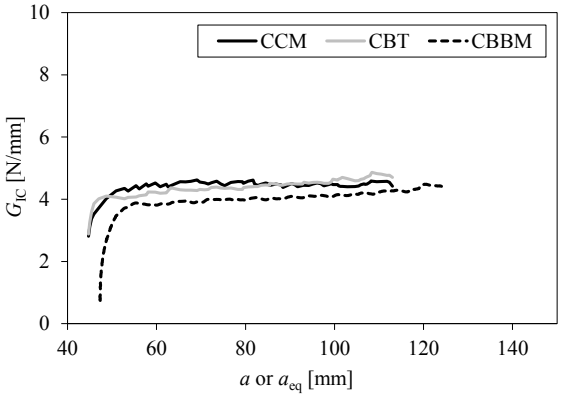

Fig. 9 - *R*-curves of a representative DCB specimen by CCM, CBT and CBBM

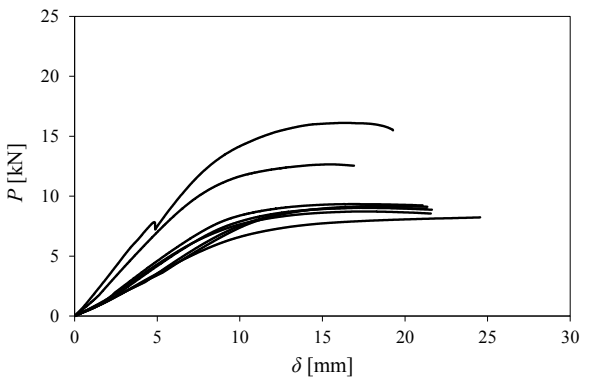

Fig. 10 - P-δ curves of the ENF specimens

It should be noted that, in toughened adhesives, at the beginning of crack growth, progressive toughening occurs by plastic deformation, possibly leading to microfissures. The curves obtained by the different methods combine reasonably well, obtaining a good steady-state G_I. As previously mentioned, the CBBM outperforms the other methods (CCM and CBT) as it is not necessary to measure a, which simplifies the analysis, and by accounting for the FPZ. Moreover, the CCM and CBT require the measurement of a, which can lead to additional errors in the G_{IC} estimates due to incorrect readings. Apart from this, the CCM also requires the estimation of dC/da by differentiating cubic polynomials adjusted to the C=f(a) curves, which constitutes another source of errors [35]. In Table 3, G_{IC} is compared between the three data reduction methods.

Table 3 - G_{IC} values obtained by the CCM, CBT and CBBM data reduction methods.

	G_{IC} [N/mm]		
Specimen	**CCM**	**CBT**	**CBBM**
1	3.87	3.78	3.52
2	4.83	4.54	4.28
3	4.34	4.33	4.18
4	4.21	3.90	4.18
5	4.83	4.47	4.48
6	4.49	4.40	4.19
Average	4.43	4.24	4.14
Standard deviation	0.37	0.32	0.33

4.4. Mode II fracture tests

Eight samples were used in the ENF tests since, in this test, unstable crack propagations can occur due to the test topology. After performing the ENF tests, the P-δ data was collected, and the results are presented in Fig. 10.

It can be concluded that the P-δ curves are in agreement, except for two specimens, which revealed a markedly different initial stiffness due to different a_0. However, this difference does not compromise the validity of the results. Typically, G_{IIC} is measured after P_m is reached and the load begins to decrease due to crack propagation, which is the proforma of the ENF tests. However, due to the high shear ductility of the adhesive, it was not possible to follow this procedure, as P did not diminish after crack initiation. As a result, it was impossible to obtain an R-curve with a steady-state value of G_{II}. Thus, G_{IIC} was considered as the value of G_{II} at the beginning of crack propagation. It should also be noticed that, when the FPZ reaches the region of the loading cylinder, the values are no longer valid for the measurement of G_{IIC}. The G_{IIC} values obtained by the different methods are shown in Table 4.

Table 4 - G_{IIC} values obtained by the CCM, CBT and CBBM

	G_{IIC} [N/mm]		
Specimen	**CCM**	**CBT**	**CBBM**
1	10.18	8.90	9.10
2	9.31	8.06	7.55
3	6.52	7.74	6.86
4	7.37	6.21	6.31
5	7.35	7.01	6.78
6	6.72	6.01	6.17
7	6.29	5.89	6.35
8	6.57	5.75	6.48
Average	7.54	6.95	6.95
Standard deviation	1.43	1.17	0.97

4.5. Discussion

Some of the obtained mechanical properties of the tensile tests were not in perfect agreement with the manufacturer's datasheet. The tensile stiffness, measured by E, resulted in 2011.76±147.14 MPa, thus giving a percentile deviation of

7.31%. An excellent agreement with the 2000 MPa specified by the manufacturer was thus obtained. Concerning σ_y, this parameter resulted in 19.41±2.84 MPa, providing a percentile deviation of 14.64 %. Since this parameter is not provided by the manufacturer, it is not possible to make a comparison. The obtained value for σ_f was 23.83±2.70 MPa, below the 30 MPa specified by the manufacturer. However, the tensile tests showed a good repeatability, since the percentile deviation on this parameter was only 11.32%, thus validating the experimental results. The obtained value of ε_f was 2.12±0.75% (percentile variation of 35.40%), whose average value is practically half of the 4% claimed by the manufacturer.

The obtained results for the TAST gives a G=713.00±54.95 MPa, with a percentile deviation of 7.7% (this value is not provided by the manufacturer). In order to calculate Poisson's ratio (ν), the parameter G can be correlated with the value of E obtained in the tensile tests, due the isotropic nature of the adhesive. Applying the well-known relation for isotropic materials, the value ν=0.41 was obtained, which fills the values described in the literature [9]. τ_y is another parameter that is not provided by manufacturer, therefore there is no way to compare this value. τ_y obtained by the shear tests was 19.87±0.65 MPa, with a percentile deviation of 3.28%. The manufacturer only provides the lap shear strength (28 MPa), which is the most approximate parameter to τ_f. The main difference from these two values is that, in the TAST test, τ_f is theoretically constant, which does not occur in a lap-shear test. The obtained τ_f was 20.35±0.82 MPa, which is lower than the lap shear value claimed by the manufacturer. Nonetheless, a good similarity between specimens was found, as it can be confirmed by the percentile standard deviation of only 4.02%. The values of γ_f reveal some scatter between specimens (5.91±0.66%, with a percentile deviation of 11.11%), which may be associated with a slight variation of t_A induced by the manufacturing process or small variations between TAST adherends. The obtained γ_f confirmed that the adhesive under analysis is ductile.

The obtained G_{IC} by the three methods were: CCM=4.43±0.37 N/mm, CBT=4.24±0.32 N/mm and CBBM=4.14±0.33 N/mm. Standard deviations were small and within the acceptable dispersion of experimentally measured quantities, with a percentile deviation of CCM=8.44%, CBT=7.47% and CBBM=7.90%. The obtained G_{IC} values for each sample were consistent between all data reduction methods, although the CBBM gives slightly lower G_{IC} compared to the other methods. However, it should be noted that the CBBM is the most reliable method as it is unaffected by possible measurement errors of a and by accounting for the FPZ effects.

The obtained G_{IIC} values, considering the three data reduction methods, were: CCM=7.54±1.43 N/mm, CBT=6.95±1.18 N/mm and CBBM=6.95±0.97 N/mm. As previously mentioned, CBBM is the most robust method, which accurately returns G_{IIC} values. Thus, it will be used as a reference value. Therefore, comparing the three methods, it can be concluded that the value achieved by the CBT is equal to the CBBM value, while the CCM has a slightly higher value. The CBBM and the CBT perfectly agree in the average G_{IIC}, whilst the CCM slightly overshoots the two other methods. However, the CCM is prone to be affected by a measurement errors and rough polynomial approximations. The percentile standard deviation for the different methods was CCM=19.01%, CBT=16.91% and CBBM=13.99%, thus within expected values.

5. Conclusions

The main objective of this work was to characterize the mechanical and fracture properties of a new polyurethane structural adhesive (SikaPower® 1277). The tensile tests resulted in E=2011.76±147.14 MPa, σ_f=23.83±2.70 MPa, σ_y=19.41±2.84 MPa and ε_f=2.1±0.75%. By comparing with the manufacturer's data sheet, it can be concluded that σ_f and ε_f are offset by a non-negligible amount from the expected values. The TAST tests allowed the estimation of G=713.00±54.95.35 MPa, τ_y=19.87±0.65 MPa, τ_f=20.35±0.82 MPa and γ_f=5.91±0.66%. The tensile fracture characterization of the adhesive, given by G_{IC} and accomplished by DCB tests, was undertaken by different data reduction methods: CCM=4.43±0.37 N/mm, CBT=4.24±0.31 N/mm and CBBM=4.14±0.17 N/mm. G_{IIC} was performed by ENF tests and it was also undertaken by the following data reduction methods: CCM=7.54±1.43 N/mm, CBT=6.95±1.18 N/mm and CBBM=6.95±0.97 N/mm. Since it is not possible to compare G_{IC} and G_{IIC} with the data spreadsheet provided by the manufacturer, it is only possible to conclude that the different methods are in accordance. This adhesive is a structural adhesive with reasonable mechanical strength as well as high ductility. As the major output of this work, the relevant mechanical and fracture properties of the SikaPower® 1277 were estimated and can now be applied for strength prediction of bonded joints by advanced modelling techniques such as CZM.

Acknowledgements

The authors would like to thank Sika® Portugal for supplying the adhesive SikaPower® 1277.

References

[1] Alfano M, Furgiuele F, Pagnotta L, et al. Analysis of fracture in aluminum joints bonded with a bi-component epoxy adhesive. *Journal of testing and Evaluation* 2010; 39: 296-303.
[2] Banea M and da Silva LF. Adhesively bonded joints in composite materials: an overview. *Proceedings of the Institution of Mechanical Engineers, Part L: Journal of Materials: Design and Applications* 2009; 223: 1-18.
[3] Banea MD, da Silva LF and Campilho RD. Moulds design for adhesive bulk and joint specimens manufacturing. *Assembly Automation* 2012; 32: 284-292.
[4] Campilho R, De Moura M and Domingues J. Stress and failure analyses of scarf repaired CFRP laminates using a cohesive damage model. *Journal of Adhesion Science and Technology* 2007; 21: 855-870.
[5] Wan Y, Wang Y, Huang Y, et al. Moisture sorption and mechanical degradation of VARTMed three-dimensional braided carbon–epoxy composites. *Composites science and technology* 2005; 65: 1237-1243.
[6] Pocius AV. *Adhesion and adhesives technology: an introduction*. Carl Hanser Verlag GmbH Co KG, 2012.
[7] Lucas F.M. da Silva SG, and Robert D. Adams. Preparing Butt joints. In: Da Silva LF, Dillard DA, Blackman B, et al. (eds) *Testing adhesive joints: best practices*. John Wiley & Sons, 2012, pp.37-42.
[8] Banea M and da Silva LF. The effect of temperature on the mechanical properties of adhesives for the automotive industry. *Proceedings of the Institution of Mechanical Engineers, Part L: Journal of Materials: Design and Applications* 2010; 224: 51-62.

[9] Da Silva LF, Öchsner A and Adams RD. *Handbook of adhesion technology*. Springer Science & Business Media, 2011.
[10] Banea MD and da Silva LF. Static and fatigue behaviour of room temperature vulcanising silicone adhesives for high temperature aerospace applications. *Materialwissenschaft und Werkstofftechnik* 2010; 41: 325-335.
[11] Campilho RD, Banea MD, Pinto AM, et al. Strength prediction of single- and double-lap joints by standard and extended finite element modelling. *International Journal of Adhesion and Adhesives* 2011; 31: 363-372.
[12] Gradin P and Nilsson S. Linear Elastic Fracture Mechanics Applied to an Adhesive Spar—Wingskin Joint. *Journal of Testing and Evaluation* 1986; 14: 326-331.
[13] Bogdanovich AE and Yushanov SP. Progressive failure analysis of adhesive bonded joints with laminated composite adherends. *Journal of reinforced plastics and composites* 1999; 18: 1689-1707.
[14] Harris J, Segall AE, Robinson D, et al. Cohesive Zone Property Measurement by a Hybrid Experimental and Numerical Method Using Ball Indentations. *Journal of Testing and Evaluation* 2015; 43: 765-775.
[15] Karac A, Blackman B, Cooper V, et al. Modelling the fracture behaviour of adhesively-bonded joints as a function of test rate. *Engineering Fracture Mechanics* 2011; 78: 973-989.
[16] Standard A. D3433-99: Standard Test Method for Fracture Strength in Cleavage of Adhesives in Bonded Metal Joints. *ASTM International, West Conshohocken* 2012.
[17] Blackman B, Kinloch A, Paraschi M, et al. Measuring the mode I adhesive fracture energy, GIC, of structural adhesive joints: the results of an international round-robin. *International journal of adhesion and adhesives* 2003; 23: 293-305.
[18] Banea M, Da Silva L and Campilho R. Mode I fracture toughness of adhesively bonded joints as a function of temperature: experimental and numerical study. *International Journal of Adhesion and Adhesives* 2011; 31: 273-279.
[19] Saldanha DFS, Canto C, da Silva LFM, et al. Mechanical characterization of a high elongation and high toughness epoxy adhesive. *International Journal of Adhesion and Adhesives* 2013; 47: 91-98.
[20] Ameli A, Papini M, Schroeder J, et al. Fracture R-curve characterization of toughened epoxy adhesives. *Engineering fracture mechanics* 2010; 77: 521-534.
[21] Azari S, Eskandarian M, Papini M, et al. Fracture load predictions and measurements for highly toughened epoxy adhesive joints. *Engineering Fracture Mechanics* 2009; 76: 2039-2055.
[22] 76-142 NT. Méthode de preparation de plaques d'adhésifs structuraux pour la réalisation d'éprouvettes d'essai de caractérisation. 1988.
[23] Monteiro JPR, Campilho RDSG, Marques EAS, et al. Experimental estimation of the mechanical and fracture properties of a new epoxy adhesive. *Applied Adhesion Science* 2015; 3: 25.
[24] ISO 11003–2: Adhesives–Determination of shear behaviour of structural adhesives–Part 2: Tensile test method using thick adherends. 2001.
[25] ISO E. 527-2: 1996. *Determination of tensile properties of plastics-Test conditions for moulding and extrusion plastics," European Committee for Standardization, Brussels, Belgium*.
[26] Da Silva LFM. Quasi-static testing of Thick Adherend Shear Test specimens". In: Da Silva LF, Dillard DA, Blackman B, et al., (eds.). *Testing adhesive joints: best practices*. John Wiley & Sons, 2012, p. 125-130.
[27] da Silva LF, Roumagnac P, Heuillet P, et al. Quasi‐Static Constitutive and Strength Tests. *Testing Adhesive Joints: Best Practices* 2012: 79-162.
[28] Campilho R, Moura D, Gonçalves DJ, et al. Fracture toughness determination of adhesive and co-cured joints in natural fibre composites. *Composites Part B: Engineering* 2013; 50: 120-126.
[29] Compston P, Jar P-Y, Burchill P, et al. The effect of matrix toughness and loading rate on the mode-II interlaminar fracture toughness of glass-fibre/vinyl-ester composites. *Composites science and technology* 2001; 61: 321-333.
[30] Standardization IOf. *ISO 15024: 2001: Fibre-reinforced Plastic Composites: Determination of Mode I Interlaminar Fracture Toughness, GIC, for Unidirectionally Reinforced Materials*. ISO, 2001.
[31] Wang Y and Williams J. Corrections for mode II fracture toughness specimens of composites materials. *Composites Science and Technology* 1992; 43: 251-256.
[32] Banea M, Da Silva L and Campilho R. Mode II fracture toughness of adhesively bonded joints as a function of temperature: experimental and numerical study. *The Journal of Adhesion* 2012; 88: 534-551.
[33] De Moura M, Campilho R and Gonçalves J. Pure mode II fracture characterization of composite bonded joints. *International Journal of Solids and Structures* 2009; 46: 1589-1595.
[34] Shahverdi M, Vassilopoulos AP and Keller T. Modeling effects of asymmetry and fiber bridging on Mode I fracture behavior of bonded pultruded composite joints. *Engineering Fracture Mechanics* 2013; 99: 335-348.
[35] De Moura M, Campilho R and Gonçalves J. Crack equivalent concept applied to the fracture characterization of bonded joints under pure mode I loading. *Composites Science and Technology* 2008; 68: 2224-2230.